Published in final edited form as:
Ultrasonics. 2005 August ; 43(8): 672–680. doi:10.1016/j.ultras.2005.03.004.

Use of multiple acoustic wave modes for assessment of long bones: Model study

Alexey Tatarinov, **Noune Sarvazyan**, and **Armen Sarvazyan***
Artann Laboratories, 1457 Lower Ferry Road, West Trenton, NJ 08618-1414, USA

Abstract

Multiple acoustic wave mode method has been proposed as a new modality in axial bone QUS. The new method is based on measurement of ultrasound velocity at different ratio of wavelength to the bone thickness, and taking into account both bulk and guided waves. It allows assessment of changes in both the material properties related to porosity and mineralization as well as the cortical thickness influenced by resorption from inner layers, which are equally important in diagnostics of osteoporosis and other bone osteopenia. Developed method was validated in model studies using a dual-frequency (100 and 500 kHz) ultrasound device. Three types of bone phantoms for long bones were developed and tested: (1) tubular specimens from polymer materials to model combined changes of material stiffness and cortical wall thickness; (2) layered specimens to model porosity in compact bone progressing from endosteum towards periosteum; (3) animal bone specimens with both cortical and trabecular components. Observed changes of the ultrasound velocity of guided waves at 100 kHz followed gradual changes in the thickness of the intact cortical layer. On the other hand, the bulk velocity at 500 kHz remained nearly constant at the different cortical layer thickness but was affected by the material stiffness. Similar trends were observed in phantoms and in fragments of animal bones.

1. Introduction

Evaluating bone condition and predicting the risk of fractures is critical for diagnostics and monitoring of osteoporosis. Unlike radiological densitometry, which determines the amount of mineralized substance in the bone volume absorbing radiation energy, the bone quantitative ultrasound (QUS) utilizes parameters of ultrasonic wave propagation through the bone medium, reflecting several physical properties of that medium.

The majority of bone ultrasonic testers are heel QUS apparatuses [1] measuring the ultrasound velocity and broadband frequency slope of attenuation by through propagation mode in the volume of *os calceus* dominantly composed of spongeous bone. Axial QUS has a special place among QUS techniques, presenting the advantage of unilateral positioning of the probe in available sites of long bones covered by a thin layer of soft tissues [2–4]. Surface transmission mode is applied and ultrasound propagates along the bone axis capturing mainly the compact bone of the cortex. The cortical thickness (CT) is one of the main determinants of ultrasonic parameters in axial propagation.

There are several axial QUS devices on the market. In Soundscan 2000, Myriad Systems Ltd., the 0.25 MHz pulse transmission is applied over a fixed distance of 50 mm to measure the longitudinal wave velocity in the tibia diaphysis. The measured velocity is highly correlated with the elasticity modulus and strength of the cortical bone [5,6], but has poor correlation with

*Corresponding author. Tel.: +609 333 0710; fax: +609 883 9080. armen@artannlabs.com (A. Sarvazyan)..

fractures risk in generalized osteoporosis [7]. The velocity in tibia at 250 kHz was shown to correlate not only with bone mineral density, but also to be affected by CT to some extent [8]. The Sunlight™ Omnisense, a multi-site system, uses a set of transducers positioned axially to measure ultrasound velocity by the so called critical angle propagation chronometry [9]. The shortest propagation time measured at 1.25 MHz along the tested bone plot corresponds to the longitudinal wave. Arguably, the major limitation of such techniques in osteoporosis diagnostics is that the fastest longitudinal component determined at relatively high frequency alone is not sensitive to processes happening in inner layers of bones.

During osteoporosis, the resorption actually starts from the endosteal surface bordering with the medullar cavity. This leads to thinning of the cortex and trabecularization of the inner cortical layer [10]. On the other hand, hypermineralization of the bone and increase of true bone mineral density noted in aged patients [11] can lead to higher ultrasound velocity in the outer layer, thus, can confound the diagnostic outcome based on the velocity alone. That is why the knowledge about changes in elastic properties and the effective thickness of the cortex are of equal diagnostic value for better assessment of different types of osteopenia and detecting osteoporosis development in long bones at earlier stages. Thinning of the cortex is one of the main indicators of decreasing total bone strength and capacity to withstand fracturing [12]. The elastic properties also can be altered by appearance of inner pores and accumulation of microcracks, as well as by degree of mineralization, i.e. by factors determining material “quality” of bone [13].

The idea of simultaneous assessment of the bone elastic properties and cortical thickness (CT) by ultrasonic measurements has been getting more and more popular in recent years. Several authors approached this problem, both experimentally and theoretically. An attempt to apply pulse-echo reflections to measure the cortical thickness was described [14]. Theoretical simulation studies on ultrasound axial propagation in model systems, confirmed by further experiments, demonstrated the possibility of ultrasonic assessment of CT by zero anti-symmetric (A0) Lamb waves [15,16]. Propagation parameters of different acoustical wave modes were investigated in acrylic plates and tubes of varying wall thickness, where experimentally determined dispersion of the A0 Lamb wave velocity was in good correspondence with the theoretical predictions [17]. The velocities of longitudinal and guided waves in tibia were compared during studies in human subjects, in which different sensitivity of these types of waves to osteoporosis [17] and bone growth [18] was revealed. Earlier, in the 1980–90s, a series of studies on bones was conducted by a Latvian group implementing “slow” type waves that they considered as an A0 Lamb or a flexural wave. The velocity was measured by point-contact transducers on short base in order to investigate in detail the long bones as non-uniform biological constructions [19–21]. The study has revealed that topographical distribution of the flexural velocity reflects distribution of CT. The topographical patterns of the velocity are known to change during aging, long-term hypokinesia and pathologies [22, 23].

This article presents a new method for bone characterization using guided and bulk ultrasound waves. The proposed approach is aimed to assess differential changes of CT and intrinsic properties of bones using multi-frequency or, at least, a dual-frequency ultrasound [24,25]. Purpose of the present study was to test sensitivity of a new dual-frequency axial QUS device developed in Artann Laboratories (NJ) using simplified models and animal bone specimens, with simulated manifestations of osteopenia. Clinical validation of the technology utility is currently underway in the pilot study.

2. Background

In general, the velocity of ultrasound is influenced by the elastic and physical properties of the bone material [26]. The equation $C = \sqrt{(E/\rho)}$, where C is ultrasound velocity; E is the elasticity modulus and ρ is the density, describes the propagation of an ultrasonic wave through an isotropic medium. However, geometrical border conditions influence ultrasound propagation and cause appearance of different modes of acoustic guided waves with geometrical dispersion of velocities. With a certain approximation, the cortical shell of a long bone can be considered as a convolved plate. Symmetric and anti-symmetric Lamb waves propagate in solid plates and have both longitudinal and shear components. Propagation velocity of the A0 Lamb wave in plates depends on the ratio of the thickness to the wavelength [27,28]. This relationship is routinely exploited in non-destructive testing [29]. In a simplified model of the bone cortical region presented as a plane layer, the A0 Lamb wave can be generated at frequencies that correspond to wavelengths much greater than the cortical thickness. As the cortical thickness increases, the velocity approaches the velocity of a surface Rayleigh wave, which is a simple function of the velocity of longitudinal waves in bone, and the Poisson ratio of the bone material.

The thickness of bones and their structural components is on a millimeter scale, just slightly smaller than the longitudinal wavelength in the range of frequencies typically used for bone assessment (0.1–1 MHz). Consequently, the propagation of acoustic waves along bones occurs in the form of various guided waves with propagation speed equally dependent on both elasticity modulus and CT. In the low frequency range (100–200 kHz) the acoustical wavelength is much greater than CT and the velocity becomes greatly dependent on the cross-sectional dimensions of the bone and its components. We shall call this wave a “low frequency guided wave” (LFGW) since definition of this wave as an A0 Lamb wave is not physically rigorous and only reflects the presence of a shear component in the induced acoustic oscillations of the bone and the specific dependence of the velocity on the thickness of the solid bone layer.

The velocity of the fastest portion of an acoustic wave with frequency over 500 kHz in bone (which we shall call a “high frequency bulk wave,” or HFBW) corresponds to a lateral compression wave having a velocity close to that of a longitudinal one propagating in infinite bulk media. The velocity of the bulk wave reflects mainly mechanical properties of the bone material, such as bulk modulus related to bone composition and mineralization. The velocity measured in this frequency range by surface transmission mode is close to the velocity of a longitudinal wave measured by through propagation.

Thus, using a combination of velocities of LFGW and HFBW simultaneously measured at two different frequencies during the same examination procedure, it might be possible to separate the contributions of the elastic properties and CT of bone. In reality, due to complex irregular and composite structure of bone, we should limit our analysis to empirical correlations with the investigated parameters.

3. Material and methods

3.1. Dual-frequency setup and measurement principle

The principle of the dual-frequency ultrasonometer developed in Artann Laboratories (NJ) is schematically illustrated in Fig. 1. Measurement of pulse propagation time in axial transmission mode was realized by a pair of ultrasonic transducers placed unilaterally on the surface of the examined object. The applied broadband transmitting and receiving transducers were designed to provide excitation and receiving of ultrasonic signals at frequencies near 100 and 500 kHz in series. To generate ultrasonic signals at the projected frequencies, a programmable waveform generator was introduced as a part of the acquisition unit based on the FLASH 100 MPIS 8051

core microprocessor C8051F124. In the present study, waveform signals were composed of sine waves at carrying frequencies of 100 and 500 kHz restricted by Gauss envelopes allowing one effective period of the carrying wave. Low and high frequency signals were obtained during one excitation-receiving act performed by synchronized digital circuits containing 32 kB FIFO memory elements. The signals were separated by time delay until full damping of the preceding signal. The sampling rate of DAC and ADC in the waveform generator and in the input amplification-digitizing circuit was 20 MHz providing discrete measurements every 0.05 μs.

The dual-frequency principle included acquisition of signals at lower and higher frequencies in broadband range applicable to bone testing in vivo in axial transmission mode. Determination of the propagation velocities related to LFGW and HFBW was performed using measured arrival times of ultrasonic pulses at 100 kHz and 500 kHz correspondingly (Fig. 2). To record the arrival times, characteristic points of signals, like those depicted in Fig. 2 zero-crossing at the first positive slope of the signal, were used. To distinguish the signal from noise and LFGW from the first arriving longitudinal wave of lower amplitude, some predetermined relative amplitude thresholds were established. The low frequency excitation was chosen at 100 kHz so that the wavelength could considerably exceed the wall thickness in the applied phantoms mimicking real CT variations in human long bones. This allowed achieving the steep slope of LFGW velocity vs. the phantom wall thickness. Due to velocity dispersion and the possible interference of different guided wave modes, it was necessary to identify the similar waveforms related to LFGW in phantoms with different thickness. For this purpose, additional experiments were made using the variable method of velocity measurements on the base distance range of 15–40 mm in the identical phantoms, and the velocity was determined from the time-distance slope. In non-uniform bone segments, the velocity was calculated at the constant base of 20 mm, as the base distance divided to time delay corrected by the transducers constant. The transducers constant was determined previously from the profiling experiments. From high frequency signals excited at 500 kHz, velocity of the HFBW was determined in the same way using the first arrival portion of the signal.

3.2. Phantoms simulating changes of cortical thickness and material properties

The variety of acoustic bone phantoms simulating variation of porosity [30,31], ultrasound propagation parameters [32,33] and bone structure [34] were previously developed by different groups. These phantoms, including the commercial ones, are bulky models appropriate for testing heel QUS devices. We had no available phantoms that mimicked atrophy processes in long bones taking into account variations of the inner bone geometry and structure. Therefore we had to develop our own simplified phantoms as well as to use fragments of natural animal bones.

Two groups of phantoms were prepared (Fig. 3):

(1) Tubular specimens modeled combined changes in material stiffness and CT, in middleshafts of long bones with no presence of the spongeous tissue. The specimens were made of available polymers and polymer composites ranging by material stiffness in the following order: ebonite, acrylic plastic, fiberglass, carbon fiber plastic. The longitudinal velocity ranged from about 2200 m/s in ebonite to 4400 m/s in carbon fiber plastic, covering the entire known range of ultrasound velocity from the poorly mineralized to hypermineralized bone. Wall thickness of the models gradually increased from 1 to 6 mm, i.e. in the range typical to the variation of CT in different human long bones.

(2) Layered specimens modeled porosity in the compact bone that progressed from the endosteum to the periosteum. Small quasi-cylindrical rubber particles with bulk velocity of about 1500 m/s modeled pores. Mixed randomly, they were incorporated

in the homogeneous solid epoxy matrix with bulk velocity of about 2700 m/s that mimicked the hard substance. Effectiveness of a similar technology was shown in earlier studies [35], in which variations of the porosity content were modeled using the similar materials. The dependence of bulk ultrasound velocity on the porosity content found in that study was in good agreement with the known dependencies of the bulk elasticity modulus on the porosity [36]. Porosity progression was modeled not only by volumetric content, but also by gradual incorporation of pores into upper layers of the cortex, thus decreasing the thickness of the solid non-porous layer from 7.5 mm to 0.5 mm step by step. The overall thickness of layered phantoms was 8 mm. Dosed porosity content in different layers ranged from 20% to 50%, representing initial stage and developed stages of osteoporosis, respectively.

3.3. Animal bone specimens

Animal bone specimens were used for testing bone tissue properties that were difficult to model in simple phantoms. Those were, firstly, the continuity of bone properties changes and CT axially from epiphysis towards diaphysis and, secondly, porosity variations in underlying spongeous layer. The specimens were prepared from animal long bones freshly obtained from a local butcher's shop. Bovine proximal tibia and porcine metacarpal bones were used. Axial fragments containing both cortical and spongeous components were obtained by longitudinal cutting of the bones. After cutting, the bones were kept in the conditions of constant humidity and temperature. CT was measured after bone cutting by a digital caliper. To account for the thickness gradient along the bone, several measurements were taken along the testing site and then averaged. Plane compact bone specimens of varied thickness were prepared by cutting thicker fragments of the bovine tibia diaphysis in order to compare results in naturally curved bone fragments and in the regularly shaped specimens.

4. Results and discussion

4.1. Tubular phantoms

Velocities of both LFGW and HFBW were measured in the tubular phantoms. A strong non-linear increase of LFGW velocity vs. wall thickness was obtained (Fig. 4A). The smaller the wall thickness or ratio of the thickness to the ultrasonic wavelength was; the sharper was the velocity gradient. The characteristic dependence of LFGW velocity on the thickness obtained in all phantoms was similar to the same dependence of the velocity of A0 Lamb waves in plates. At 100 kHz, the LFGW velocity slope is very steep with a velocity gradient of 200–400 m/s per 1 mm increment over the thickness range of 1–2.5 mm. Thus, at a measurement accuracy of 20–30 m/s, changes in CT on the order of 0.1 mm can be revealed in the sites of thin cortex. In large human bones, e.g. tibia and radius, such CT values are usually met in metaphyseal zones. In these sites our method can potentially show the highest resolution and the best sensitivity to the resorption onset. In the thickness range of 2.5–6 mm, the gradient of the velocity slope decreases to 40–60 m/s per 1 mm. Even in this case, the method can be sensitive enough to discriminate bones with thinner or thicker cortex with resolution about of 0.5–1 mm.

The HFBW velocity at 500 kHz (Fig. 4B) was evaluated as a function of phantom's wall thickness and material stiffness. It did not change substantially with variation of the wall thickness in phantoms made from hard materials, like fiberglass and carbon fiber plastic, where ultrasound velocity was close to that in normal bone tissue. In softer materials such as ebonite and acrylic plastic, where the velocity was about 2500 m/s or less corresponding to the ultrasound velocity in demineralized or poorly mineralized bone [37], the HFBW velocity started to decrease significantly at thicknesses 2 mm and less. At wall thicknesses of 2.5 mm and higher, deviations of the HFBW velocity did not exceed the measurement error.

Obtained LFGW and HFBW velocities were distributed according to material stiffness, from the softest, ebonite, to the stiffest, carbon fiber plastic. For the LFGW the stiffness in phantoms can be compared only at equal thicknesses. The stiffness of the bone material is best calculated from HFBW in the diaphysis where the cortex is relatively thick. The LFGW velocity, normalized by the elastic modulus or by the HFBW velocity, can be an indicator of CT changes. In sites with thin and poorly mineralized tissue, such as epiphyseal regions in children, influence of CT on the velocities of both LFGW and HFBW should be taken into account.

The experiment demonstrated that the geometric dispersion phenomenon previously considered for plates, can be extended for assessment of CT in tubular bones or more complicated tubular shells using empirically established correlations.

4.2. Layered porous phantoms mimicking progressing porosity from inner layers

Fig. 5 presents LFGW and HFBW velocities in the layered porous phantoms simulating progressing porosity from the inner (endosteum) side of the cortex. The measurements were produced from the side of an intact epoxy matrix (outer non-porous layer) by positioning the transducers unilaterally on the upper (outer) surface. Effective thickness of this intact layer was gradually decreased by proportional increase of the porous layer from Phantom #1 (pure solid epoxy) to Phantom #6, in which porous inclusions almost reached the very upper surface. The LFGW constantly decreased from Phantom #1 to Phantom #6. Decreasing the thickness of the intact layer by 1 mm led to a 50 m/s decrease in LFGW velocity, on average. Thus, it was demonstrated that an ultrasonic guided wave at low frequency is able to provide information about deeper layers and that the velocity could be highly sensitive to the porosity progressing from endosteum at early stages of osteoporosis. A significant decrease in HFBW velocity was noted only in Phantom #6, where the porosity reached the outer layer and the thickness of the solid epoxy surface layer was not greater than 0.5 mm. In Phantoms #1–5, HFBW velocity was approximately constant and equal to the bulk velocity in epoxy. The ratio of the velocities of LFGW and HFBW was about 0.5 in the solid epoxy phantom and decreased gradually to about 0.25 in the phantom with the thinnest solid layer. From this, it can be concluded that the LFGW is a surface wave in Phantom #1, but transforms into an A0 Lamb wave by thinning of the solid layer.

4.3. Axial bone fragments

By moving from epiphysis towards diaphysis, the cortical thickness in long bones increases several times from a fraction of a millimeter to several millimeters, that has a significant impact on LFGW velocity. Fig. 6A presents axial profiles obtained from the axial fragment of bovine tibia with intact and removed spongy component. Continuous increase of CT from 1.5 to about 7 mm along the bone was followed by a rise of LFGW velocity by more than a factor of two —from about 700 to 1500 m/s. Removal of the deeper spongeous component caused some decrease of the velocity in the epiphysis, where the cortical layer is very thin and there is no distinct partition between the spongy and compact components. The dependence of the velocity on the CT, obtained by discrete measurements along the bone, was found to be characteristic of an A0 Lamb wave (Fig. 6B). The dependence graphs obtained in the flat bone specimens of regular thickness and in the axial bone fragment have similar character that confirms the close nature of the ultrasonic wave in these objects. A slight shift of the graph from flat specimens to upper values can be explained by greater material stiffness of the bone in diaphysis, from which the specimens were cut.

Young and adult bones admittedly differ in both geometry and tissue material properties due to different size and degree of ossification. To compare young and adult bones, two porcine metacarpal bones were examined: the first one from a 10-month-old adult and the second one from a 3-month-old piglet. Axial distribution profiles of the CT and ultrasound velocities of

LFGW and HFBW are presented in Fig. 7A–C. The cortex in the adult animal bone was about 2 times thicker (averaged over the bone's length) than in the young one (A). The ultrasound velocities of LFGW (B) and HFBW (C) differed not only in their magnitudes (2.5–3 times) but also by different distribution patterns along the bones. The LFGW velocities (for any given CT) were much lower in young animal. Lowered HFBW velocity was noted only in the physis zone. Incomplete ossification in this area of the piglet's bone was the reason that the HFBW velocity there was much lower than in the corresponding area of the adult bone. In the diaphyseal part, where the bone is completely mineralized and mature, the HFBW velocities were at maximum about 4000 m/s and approximately similar in the adult and young animals.

4.4. Underlying spongeous bone

The possibility to assess changes in trabecular bone in epiphyseal and metaphyseal regions of long bones by LFGW was tested using isolated fragments from the proximal part of bovine tibia. Prepared specimens contained both cortical and spongy components with thinner (1.5 mm) and thicker (3 mm) cortex. To simulate an increased porosity in underlying spongeous bone, random 1 mm diameter pores were drilled through the specimen in spongeous tissue, taking approximately 50% of the total volume. The pores were filled with physiological solution. Comparison of LFGW velocity in intact and drilled specimens is presented in Fig. 8. The significantly lowered values were found in a specimen after drilling spongy bone resulting in thinner cortex. This result provides evidence of a complex influence of the cortical and trabecular components on ultrasound velocity at low frequency, if the wavelength significantly exceeds the CT. Much smaller changes in HFBW velocity were found with 1.5 mm cortex, and practically no changes were found with 3 mm cortex.

5. Conclusion

A dual-frequency method has been proposed as a new modality in axial bone ultrasonometry based on measuring velocities of ultrasound at different wavelength ratios to the bone thickness and applying bulk and guided waves. A low frequency of 100 kHz can be applied to measure the velocity of a guided wave in bone, having similar dependence on the thickness as the zero anti-symmetric Lamb wave in plates. In a higher frequency band (0.5–1 MHz) the first propagating wave mode has the same velocity as a bulk longitudinal wave. Measuring velocities of both types of waves, provides a possibility to discern contributions of the material properties and the cortical thickness. Applying a low frequency guided wave makes it possible to assess changes in spongeous bone layer underlying a thin cortex. The model studies in simplified phantoms, simulating changes of the cortical thickness, porosity developed from deep lying layers under the outer surface of the cortex and differences in material properties, prove feasibility of the approach. The major trends observed in the phantoms were confirmed by data obtained from fragments of animal bones. The proposed method could be used for diagnostics of bone condition if the contribution of soft tissues and topographical heterogeneity in real bones are considered. It has a potential for better detection of the early stage of osteoporosis in long bones by assessing changes of the cortical thickness along the bone and changes in deep underlying spongy layers in metaphyseal zones. The new QUS device, utilizing the dual-frequency ultrasound method for quantitative bone characterization in humans, currently undergoes validation in investigational clinical study. The results of this study will be published upon its completion.

Acknowledgments

This work was supported in parts by the NIH grant 2R44AG17400 and NASA grant NAS3 02167.

References

[1]. Gregg EW, Kriska AM, Salamone LM. The epidemiology of quantitative ultrasound: a review of the relationships with bone mass, osteoporosis and fracture risk. Osteopor. Int 1997;7:89–99.

[2]. Hans, D.; Bo, F.; Fuerst, T. Non-heel quantitative ultrasound devices. In: NJeh, CF.; Hans, D.; Fuerst, T.; Gluer, CC.; Genant, HK., editors. Quantitative Ultrasound: Assessment of Osteoporosis and Bone Status. Martin Dunitz; London: 1999. p. 145-162.

[3]. Camu E, Talmant M, Berger G, Laugier P. Analysis of the axial transmission technique for the assessment of skeletal status. J. Acoust. Soc. Am 2000;108:3058–3065. [PubMed: 11144598]

[4]. Lowet G, Van der Perre G. Ultrasound velocity measurement in long bones: Measurement method and simulation of ultrasound wave propagation. J. Biomech 1996;29:1255–1262. [PubMed: 8884471]

[5]. Lee SC, Coan BS, Bouxsein ML. Tibial ultrasound velocity measured in situ predicts the material properties of tibial cortical bone. Bone 1997;7:119–125. [PubMed: 9213018]

[6]. Foldes AJ, Rimon A, Keinan DD, Popovtzer MM. Quantitative ultrasound of the tibia: a novel approach for assessment of bone status. Bone 1995;17:363–367. [PubMed: 8573409]

[7]. Bouxsein ML, Coan BS, Lee SC. Prediction of the strength of the elderly proximal femur by bone mineral density and quantitative ultrasound measurements of the heel and tibia. Bone 1999;25(1): 49–54. [PubMed: 10423021]

[8]. Prevrhal S, Fuerst T, Fan B, Njeh C, Hans D, Uffmann M, Srivastav S, Genant H. Quantitative ultrasound of the tibia depends on both cortical density and thickness. Osteopor. Int 2001;12:28–34.

[9]. Hans D, Weiss M, Fuerst T, Kantorvich E, Singel C, Genant H. A new reflection quantitative ultrasound system: preliminary results of multi site bone measurements. Osteopor. Int 1997;7(3): 175.

[10]. Keshwarz NM, Recker RR. Expansion of the medullary cavity at the expense of cortex in postmenopausal osteoporosis. Metab. Bone Dis. Relat. Res 1984;5:223–228. [PubMed: 6493034]

[11]. Vajda EG, Bloebaum RD. Age-related hypermineralization in the female proximal human femur. Anat Rec. 1 1999;255(2):202–211.

[12]. Turner CH. Biomechanics of bone: determinants of skeletal fragility and bone quality. Osteopor. Int 2002;13(2):97–104.

[13]. Ammann P, Rizzoli R. Bone strength and its determinants. Osteopor. Int 2003;14(Suppl 3):S13–S18.

[14]. Wear KA. Autocorrelation and cepstral methods for measurement of tibial cortical thickness. IEEE Trans. Ultrason Ferroelectr. Freq. Contr 2003;50(6):655–660.

[15]. Bossy E, Talmant M, Laugier P. Effect of bone cortical thickness on velocity measurements using ultrasonic axial transmission: a 2D simulation study. J. Acoust. Soc. Am 2002;112(1):297–307. [PubMed: 12141355]

[16]. Lefebvre F, Deblock Y, Campistron P, Ahite D, Fabre JJ. Development of a new ultrasonic technique for bone and biomaterials in vitro characterization. J. Biomed. Mater. Res. (Appl. Biomater.) 2002;63:441–446.

[17]. Nicholson PH, Moilanen P, Karkkainen T, Timonen J, Cheng S. Guided ultrasonic waves in long bones: modelling, experiment and in vivo application. Physiol. Meas 2002;23(4):755–768. [PubMed: 12450274]

[18]. Moilanen P, Nicholson PHF, Karkkainen T, Wang Q, Timonen J, Cheng S. Assessment of the tibia using ultrasonic guided waves in pubertal girls. Osteopor. Int 2003;14:1020–1027.

[19]. Janson HA, Tatarinov AM, Dzenis VV, Kregers AF. Constructional peculiarities of the human tibia defined by reference to ultrasound measurement data. Biomaterials 1984;5:221–226. [PubMed: 6487702]

[20]. Tatarinov AM, Dzenis VV, Yanson HA. Acoustic anisotropy of human tubular bones. Mech. Compos. Mater. New York 1985;21(1):124–131.

[21]. Yanson HA, Dzenis VV, Kregers AF, Oga MV, Tatarinov AM. Structural features of human tubular bones relative to ultrasound. Mech. Compos. Mater. New York 1983;19(4):542–549.

[22]. Tatarinov AM, Dzenis VV, Yanson HA. Role of compact bone tissue thickness in the investigation of tubular bones by ultrasonic exponential concentrators. Mech. Compos. Mater. New York 1985;21 (2):342–357.

[23]. Tatarinov AM, Dubonos SL, Yanson HA, et al. Ultrasonic diagnostics of human bone state during 370-day antiortostatic hypokinesia. Space Biol. Aerospace Med 1990;2:29–31. in Russian, ann. in Engl.

[24]. Sarvazyan, A.; Tatarinov, A. Method and device for multi-parametric ultrasonic assessment of bone conditions. US patent. 6,468,215 B1. 2001.

[25]. Tatarinov, A.; Sarvazyan, A. Dual-frequency method for ultrasonic assessment of bones: model study. Proceedings of the World Congress on Ultrasonics; September 2003; p. 895-898.CDROM

[26]. Njeh, CF.; Nicholson, PHF.; Langton, CM. The physics of ultrasound applied to bone. In: NJeh, CF.; Hans, D.; Fuerst, T.; Gluer, CC.; Genant, HK., editors. Quantitative Ultrasound: Assessment of Osteoporosis and Bone Status. Martin Dunitz; London: 1999. p. 67-76.

[27]. Meeker, TR.; Meitzler, AH. Guided wave propagation in elongated cylinders and plates, in: Physical Acoustics: Principles and Methods. In: Mason, WP., editor. Methods and Devices, Part A. Vol. vol. I. Academic Press; NY: 1964.

[28]. Viktorov, IA. Rayleigh and Lamb Waves, Physical Theory and Applications. Plenum Press; New York: 1967.

[29]. Chimenti DE. Guided waves in plates and their use in materials characterization. Appl. Mech. Rev 1997;50:247–284.

[30]. Clarke AJ, Evans JA, Truscott JG, Milner R, Smith MA. A phantom for quantitative ultrasound of trabecular bone. Phys. Med. Biol 1994;39:1677–1687. [PubMed: 15551538]

[31]. Strelitzki R, Evans JA, Clarke AJ. The influence of porosity and pore size on the ultrasonic properties of bone investigated using a phantom material. Osteopor. Int 1997;7(4):370–375.

[32]. Njeh CF, Richards A, Boivin CM, Hans D, Fuerst T, Genant HV. Factors influencing the speed of sound through the proximal phalanges. J. Clin. Densitom 1999;2(3):241–249. [PubMed: 10548820]

[33]. Quantitative Ultrasound Phantom: Tissue Equivalent, Calibration Standard. Available from: <http://www.cirsinc.com/products/model063.html>

[34]. Langton CM, Whitehead MA, Langton DK, Langley G. Development of a cancellous bone structural model by stereolithography for ultrasound characterisation of the calcaneus. Med. Eng. Phys 1997;19(7):599–604. [PubMed: 9457693]

[35]. Tatarinov A, Pontaga I, Vilks U. Modeling the influence of mineral content and porosity on ultrasound parameters in bone by using synthetic phantoms. Mech. Compos. Mater 1999;35:147–154.

[36]. Martin RB. Determinants of the mechanical properties of bones. J. Biomech 1991;24:79–88. [PubMed: 1842337]

[37]. Tavakoli MB, Evans JA. Dependence of the velocity and attenuation of ultrasound in bone on the mineral content. Phys. Med. Biol 1991;36(11):1529–1537. [PubMed: 1754623]

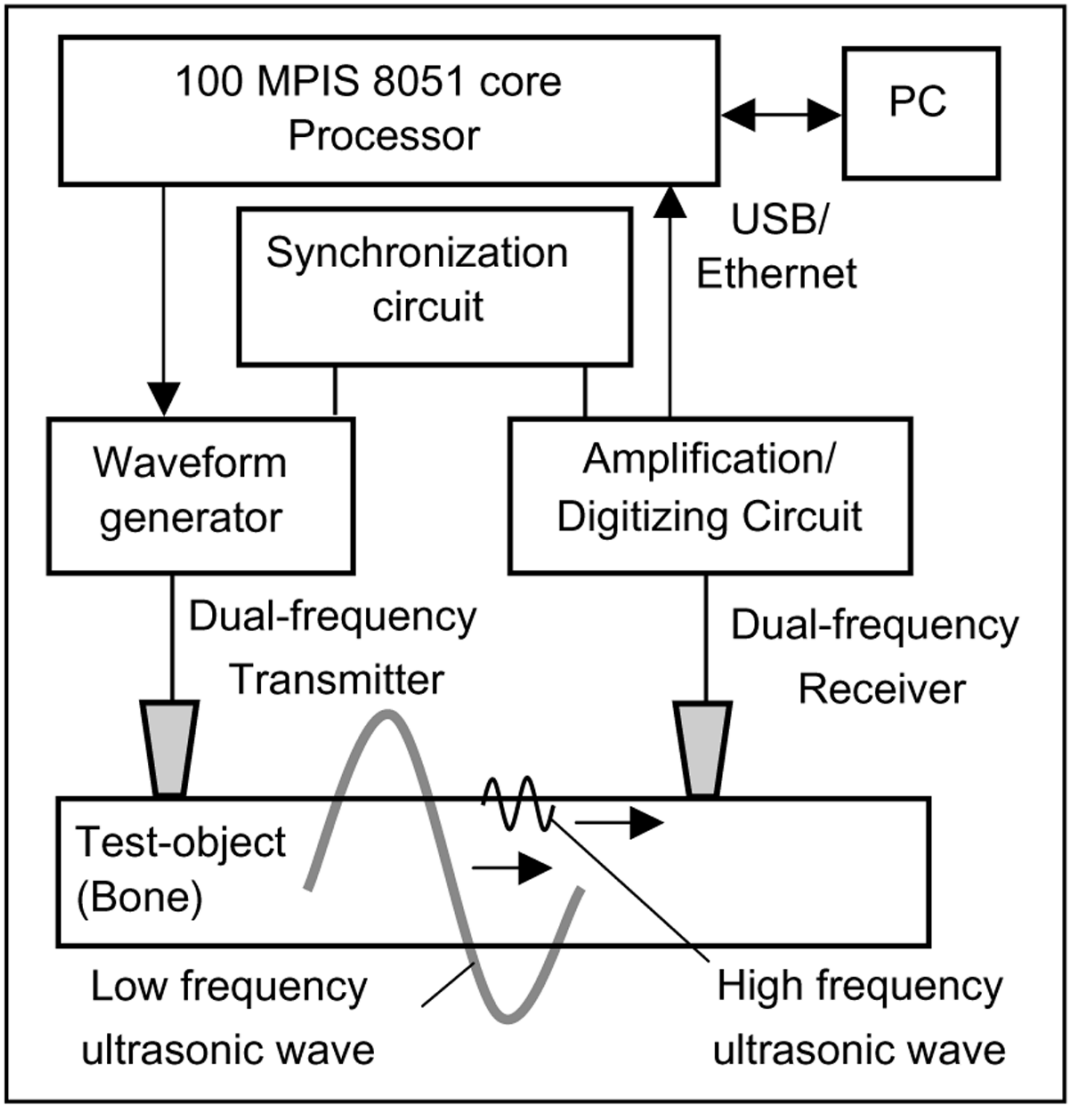

Fig. 1.
General principle of dual-frequency ultrasonometer.

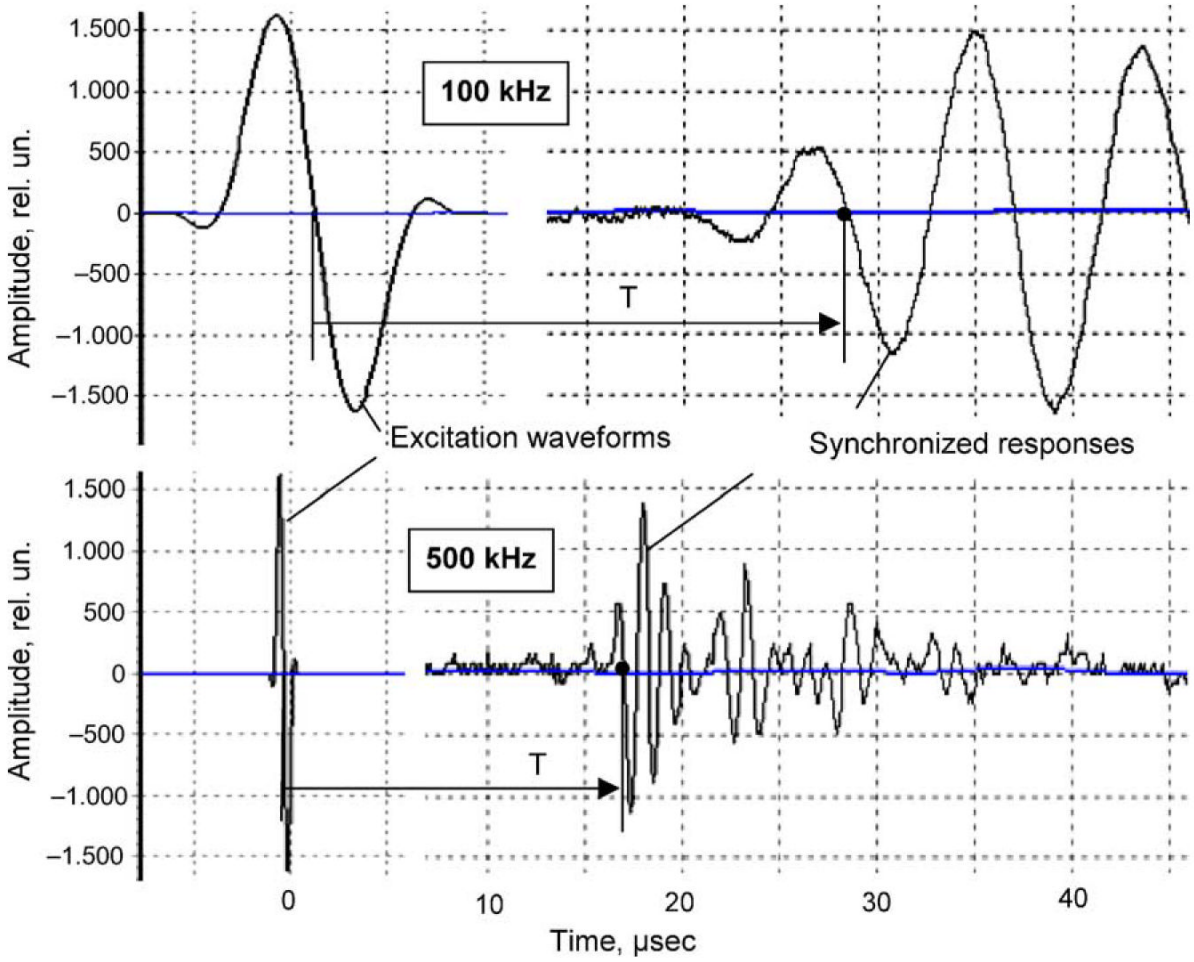

Fig. 2.

Excitation and acquisition of low- and high-frequency ultrasonic signals: black dots show points of signals used for detection of pulse arrival times *T*.

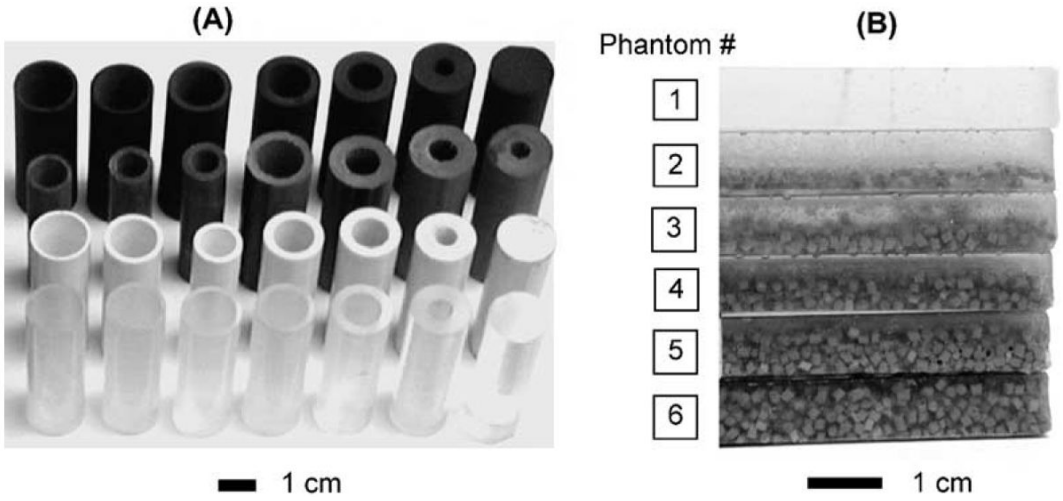

Fig. 3.
Phantoms: tubular (A) and layered with pores (B).

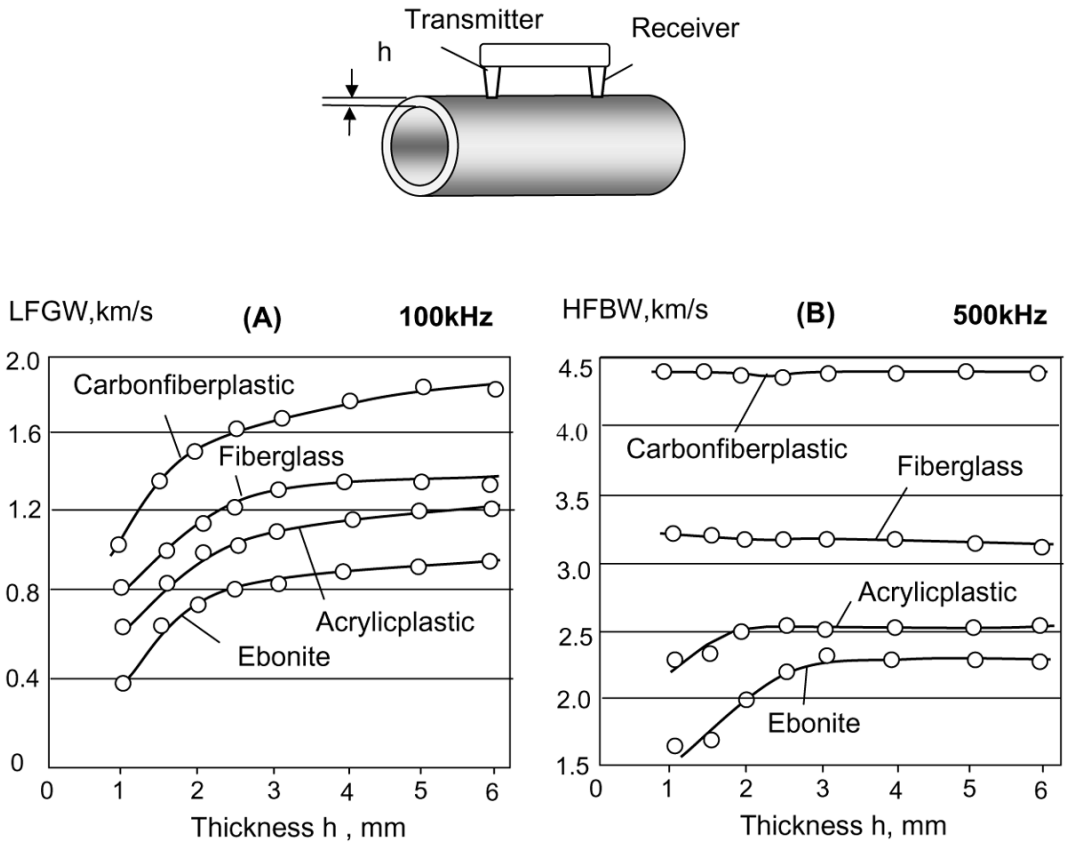

Fig. 4.

Dependence of velocities of LFGW (A) and HFBW (B) waves obtained at 100 and 500 kHz, correspondingly, on wall thickness (*h*) in tubular phantoms made of materials with gradually varied elasticity modulus.

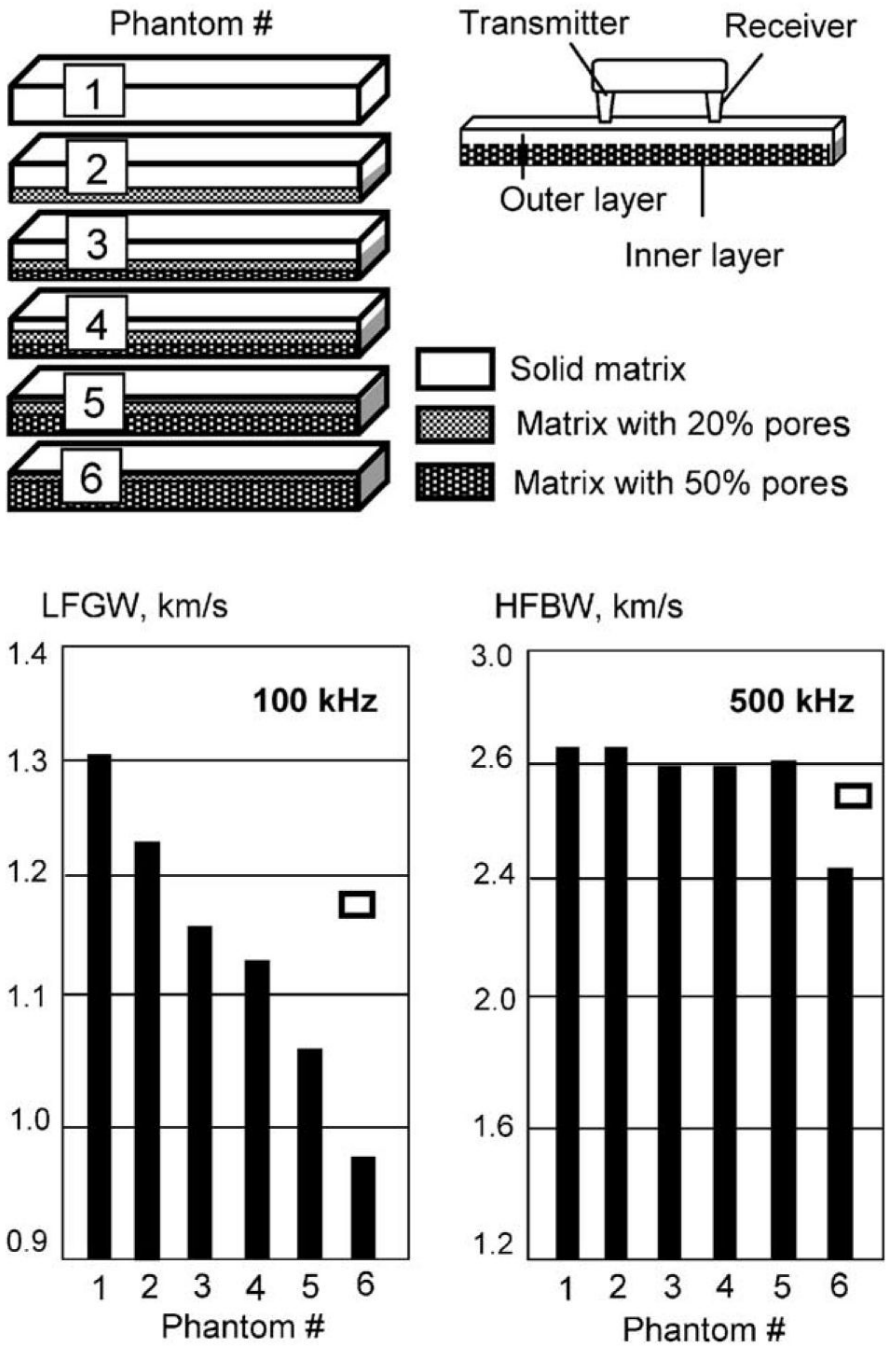

Fig. 5.

Changes of velocities of LFGW and HFBW obtained at 100 and 500 kHz, respectively, in phantoms mimicking increasing porosity from the inner layer of compact bone. Measurement error is shown by rectangles in the graphs.

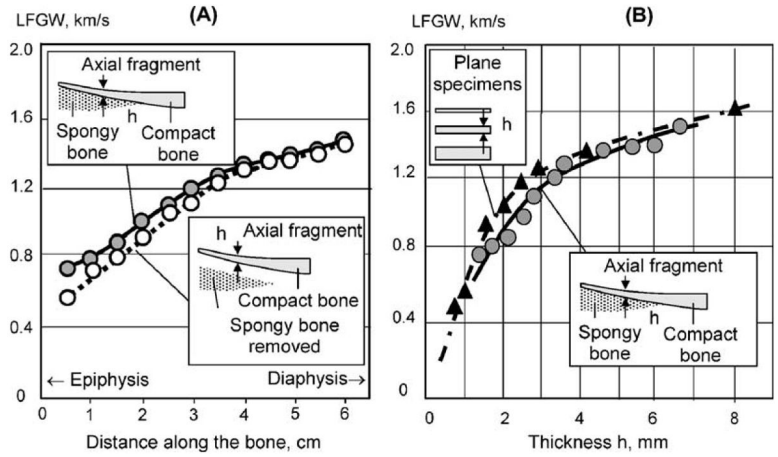

Fig. 6.

Results of measurements in bone fragment: A—axial graphs of LFGW velocity before and after removal of spongeous component; B—dependence of LFGW velocity on bone thickness obtained in intact bone and in regular shape specimens.

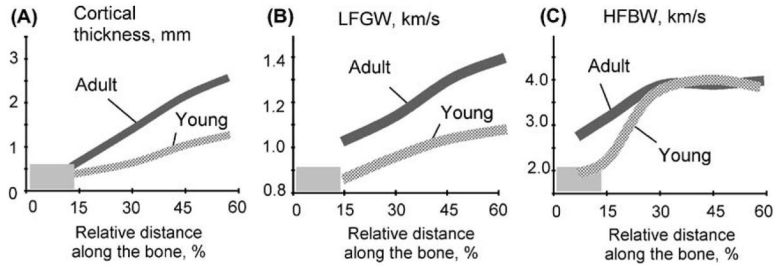

Fig. 7.

Axial graphs of cortical thickness (A), and ultrasound velocities related to LFGW (B) and HFBW (C) obtained at 100 and 500 kHz, correspondingly, in adult and young porcine metacarpal bones.

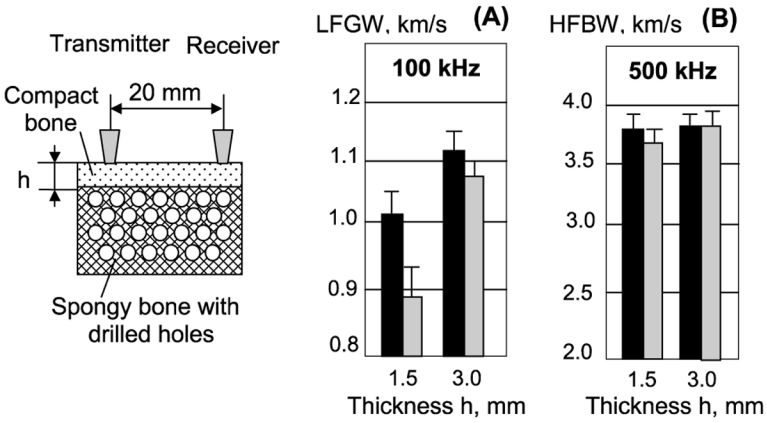

Fig. 8.

Velocities of LFGW (A) and HFBW (B) waves measured at 100 and 500 kHz in composite bone specimens before and after simulated increase of porosity in spongeous component.